THE ASTROPHYSICAL JOURNAL, Vol. 152, April 1968

EVOLUTION OF MASSIVE HELIUM-BURNING SUPERGIANTS

RICHARD STOTHERS AND CHAO-WEN CHIN
Institute for Space Studies, Goddard Space Flight Center, NASA, New York
Received July 27, 1967

ABSTRACT

Models have been constructed for massive stars of 15, 60, and 100 $M_\odot$ in the core helium-burning phase of evolution Their luminosity remains nearly constant during evolution and is relatively insensitive to uncertainties in the interior structure, whereas the effective temperature is definitely not Previously published models in which the opacity was taken to be only electron scattering or in which the envelope instability was treated as fully convective start helium burning as blue supergiants With the inclusion of bound-free absorption and semiconvective mixing, the models start as red supergiants, then move to the blue region The effective temperature of blue supergiants may also be lowered by increasing the hydrogen, metals, and/or CNO abundances. The fraction of time spent in the blue region and the maximum effective temperature attained are probably both larger at higher masses. However, these are very sensitive to conditions in the previous red-supergiant phase. Subsequent to the blue phase, the stars are expected to burn carbon (in a second red-supergiant phase) We suggest that the red supergiants in young clusters like h and χ Per may be, at least in part, in the core helium-burning phase of evolution.

I. INTRODUCTION

The precise location of the luminous supergiants on the H-R diagram can shed considerable light on the state of their interior structure. This was shown in a preliminary way by Hayashi and Cameron (1962), who found that the blue-supergiant branch of h and χ Persei could be explained by core helium-burning stellar models.

In order to obtain more detailed information on the brightest supergiants, evolutionary tracks during core helium burning have been computed for 15 $M_\odot$ and two heavier masses. Comparison of these tracks with the observational H-R diagram then yields, at least in principle, some limits to the extent of internal mixing, the rate of mass loss, and the initial chemical composition.

II. ASSUMPTIONS

The masses which have been calculated are 15, 60, and 100 $M_\odot$, with

$$X_e = 0.70,\ Y_e = 0.27,\ Z_e = 0.03,\ X_{\rm CNO} = Z_e/2\ .$$

The hydrogen-burning phase for these masses has been determined previously (Stothers 1965, 1966*b*). Since the intervening phases up to the onset of helium burning may be neglected (Hayashi and Cameron 1962; Stothers 1966*a*), the initial core helium-burning stage has been calculated from the known run of chemical composition at the end of core hydrogen burning:

$$\begin{aligned} X &= X_e && (q > q_0)\ , \\ X &= a_0 + a_1 q + a_2 q^2 && (q_0 \geq q \geq q_s)\ , \\ X &= 0 && (q < q_s)\ . \end{aligned}$$

The coefficients a_i and q_0 are determined from the last core hydrogen-burning model for each mass. The hydrogen shell source is initially placed at a mass fraction q_s corresponding to a hydrogen abundance of $X_s = 0.03$; the shell is approximated by a discontinuous jump in chemical composition and luminosity. Semiconvective mixing is taken into account in the manner described earlier (Stothers 1966*a*). The opacity is assumed, as

before, to be due solely to electron scattering. Corrections to the models, due to our neglect of bound-free absorption, are calculated afterward. The over-all structure, as well as the other assumptions, notations, and nuclear-energy parameters, are the same as in Stothers (1966*a*).

Calculation of the evolutionary sequences of models has proceeded along the lines used for a star of 30 $M_\odot$ calculated earlier (Stothers 1966*a*). A detailed study of the limitations of the models is given for the sequence at 15 $M_\odot$, described in the next section.

TABLE 1

MODELS FOR 15 $M_\odot$ DURING CORE HELIUM DEPLETION

	15 $M_\odot$								
	1	2	3	4	5	6	7	8	9
Y	0 970	0 844	0 576	0 408	0 307	0 184	0 0594	0 0307	0 0084
X_C	0 000	0 124	0 369	0 504	0 568	0 606	0 512	0 440	0 358
Sequence A:*									
q_s	0 220	0 280	0 320	0 335	0 342	0 350	0 357	0 359	0 361
X_s	0.030	0 229	0 352	0 395	0 415	0 437	0 457	0 463	0 468
L_H/L	0 885	0.764	0 612	0 516	0 457	0 379	0 301	0 286	0 282
q_4	0 090	0 136	0 177	0.197	0 208	0 221	0 235	0 239	0 241
log T_c	8 211	8 235	8 264	8 286	8 302	8 329	8 377	8 401	8 440
log ρ_c	3 122	3 028	3 006	3 025	3 047	3 100	3 216	3 283	3 394
log $(L/L\odot)$	4 906	4 922	4 935	4 942	4 946	4.952	4 963	4 967	4 975
log T_e	4 080	4 209	4 295	4 317	4 323	4 321	4 299	4 281	4 244
τ (10^5 yr)	0 00	1 69	4 59	6 26	7 22	8 47	10 05	10 55	10 98
Sequence B:†									
q_s	0 220	0 280	0 320	0 335	0.342	0 350	0 357	0 359	0 361
X_s	0 030	0 229	0 352	0 395	0 415	0 437	0 457	0 463	0 468
log $(L/L\odot)$			4 86	4.87	4 88	4 89	4 90	4 90	4 90
log T_e	conv.	conv.	4 10	4 16	4 17	4 17	4 13	4 09	3 98
Sequence C:‡									
q_s	0 220	0 220	0 220	0 220	0 220	0.220	0 220	0 220	0 220
X_s	0 600	0 600	0 600	0 600	0 600	0 600	0 600	0 600	0 600
log $(L/L\odot)$	4.77	4 77	4 77	4 77	4 77	4 77	4 77	4 77	4 78
log T_e	4 38	4 39	4 39	4 40	4 40	4.40	4 39	4 38	4 37

* Sequence A: $\kappa = \kappa_s$; $q_0 = 0\,454$; $X(q) = -0\,865 + 4\,65q - 2\,65q^2$.

† Sequence B: $\kappa = \kappa_s + \kappa_a$; q_0 and $X(q)$ same as for A.

‡ Sequence C: $\kappa = \kappa_s + \kappa_a$; $q_0 = 1$; $X(q) = 0\,600$.

III. INVESTIGATION OF 15 $M_\odot$

It is well known that the radius (and hence location on the H-R diagram) of stars with radiative envelopes and nuclear-burning shells is rather sensitive to physical uncertainties and assumptions. In the following, we shall discuss these uncertainties in the case of our models for 15 $M_\odot$ (Table 1). For comparison, we have also the models of Hayashi and Cameron (1962) for 15.6 $M_\odot$ and of Iben (1966*b*) for 15 $M_\odot$, who used different assumptions and chemical compositions.

a) Opacity and Mixing

With electron scattering as the sole opacity source, models of very massive stars begin helium burning as hot (blue) supergiants. This follows from our results for 15 $M_\odot$ (sequence A in Fig. 1) and higher masses, as well as from the earlier results of Hayashi and Cameron (1962) for 15.6 $M_\odot$ and of Stothers (1966*a*) for 30 $M_\odot$.

A striking change occurs, however, if bound-free absorption is included in the model

calculations. We have taken this extra source of opacity into account by replacing the envelope parameter C (Stothers 1963*a*) with

$$C' = C\left(1 + \frac{\kappa_a}{\kappa_s}\right),$$

where κ_a is approximated by Kramers' law with $t/\tilde{g} = 1$ (e.g., Schwarzschild 1958):

$$\kappa_a = \frac{1330}{T^{1/2}} \frac{\mu\beta}{1-\beta} Z(1+X), \qquad \kappa_s = 0.19(1+X).$$

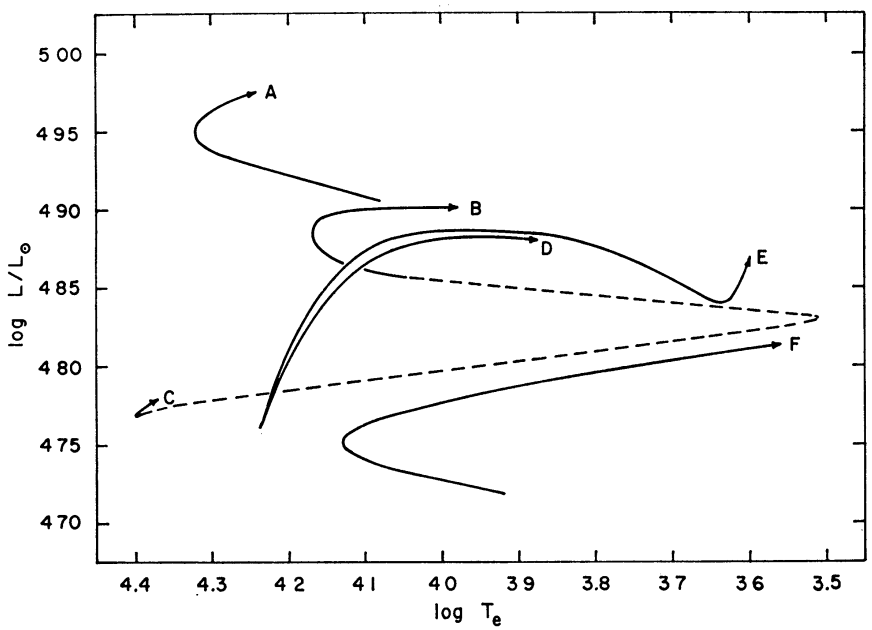

FIG. 1.—Theoretical H-R diagram for stars of 15 $M_\odot$ during the phase of core helium burning. Stars reach the onset point (tail of the arrows) coming from the *left* of the diagram where the main sequence lies. The final point (head of the arrows) occurs at the stage when $Y_c = 0.01$. The evolutionary tracks are due to: this paper (Table 1) for *A*, *B*, and *C;* Iben (1966*b*) for *D* and *E;* and Hayashi and Cameron (1962) for *F*. The dashed segments are schematic only. See text for explanations.

To calculate T at each point in the envelope integration, we require another eigenvalue, the total radius R. It turns out that κ_a is important only in the outermost part of the envelope and therefore does not have a large effect on the core evolution. To estimate its effect on the radius, we have assumed the same q_s, $X(q)$, and central values of Y and X_C as those given for the purely electron-scattering models. Then the resulting changes on the H-R diagram are shown in Figure 1 (sequence *B*). The dashed segment of the evolutionary track has not been explicitly calculated and is only schematic.

Clearly, the inclusion of bound-free absorption has drastic consequences for the radius. When helium burning commences in the core, the star is a cool (red) supergiant (cf. Table 1). However, as the mass fraction of the hydrogen-burning shell increases during the early stages of core helium burning, the effect of the bound-free absorption is reduced. The star rapidly moves into the region of blue supergiants. We have not attempted to estimate the depth to which mixing takes place in the convective envelope when the star is a red supergiant. The extent of convection will depend on the convective efficiency in the outermost layers of the star; even with the present mixing-length theory, considerable uncertainty will exist in the determination of the inner boundary of the

convective region. However, judging from the results for a star of 9 $M_\odot$ (Iben 1966*a*), we believe that the convection will not extend below the hydrogen-burning shell for 15 $M_\odot$. Therefore our core models should be approximately valid.

Nevertheless, the effective temperature of the surface will be uncertain, depending rather strongly on the distribution of hydrogen and helium in the envelope. In the above, we assumed that the convective mixing in the envelope during the red-supergiant phase would cover less than 55 per cent of the total mass ($q > q_0$), so that the composition gradient in the intermediate zone remained unaltered. As an extreme alternate possibility, we now consider that convection has mixed the envelope all the way to the original hydrogen shell source. Thus 78 per cent of the mass will have been covered by envelope convection. Since the total amount of hydrogen must be conserved, the homogeneous mixture above the discontinuity at the shell source is characterized by $X_e = 0.60$ and $Z_e = 0.03$. Now the amount of hydrogen depletion during core helium burning will be approximately $-\Delta\int X dq = 0.036$, implying an increase in mass fraction of the shell equal to $\Delta q_s = 0.06$. Since this increase is relatively small, and since the stellar structure is much more sensitive to the mean molecular weight of the core material, we have recalculated the models for 15 $M_\odot$, assuming a constant q_s, an $X(q) = 0.60$, and the central values of Y and X_C given for the purely electron-scattering models. The resulting track on the H-R diagram is shown in Figure 1 (sequence *C*). Again, the dashed segment is schematic only.

The evolutionary tracks for 15 $M_\odot$ determined here differ in one important respect from the tracks determined by Iben (1966*b*). Our models begin core helium burning in the red-supergiant region; Iben's models start in the blue-supergiant region (sequences *D* and *E* in Fig. 1). The reason for the difference lies solely in the mode of mixing within the intermediate zone that is initially assumed during core hydrogen burning. Iben assumed that the mixing is fully convective, and therefore obtained a *homogeneous* composition in the intermediate zone, with a composition jump at the interface with the outer, unmixed part of the envelope. Such a distribution of composition has two effects. First, the large-scale homogenization in the star tends to make the effective temperature hotter than in the case where the intermediate zone has a gradient of mean molecular weight. Second, the high hydrogen abundance at the shell results in only a small outward growth of the shell mass fraction during core helium burning; this produces an evolutionary track which runs slightly to the right, without a turnback, on the H-R diagram.

However, it seems quite certain on simple theoretical grounds that the intermediate zone (whose unstable boundary moves steadily out into the unmixed envelope) cannot be fully convective, for reasons analogous to those given by Sakashita, Ôno, and Hayashi (1959). The treatment of the unstable region as semiconvective in the Sakashita-Hayashi mode (which we have adopted) or in the Schwarzschild-Härm mode gives results nearly the same as if the region were treated as wholly radiative. The reason is simply the similar distributions of hydrogen and helium which are set up. The possible effect of rotationally induced mixing has not been investigated.

b) Nuclear-Energy Generation

The models of the bluest supergiants, where $Y_c \sim 0.3$ and electron scattering dominates as the opacity source, are relatively insensitive to moderate adjustments in the nuclear-energy sources. For example, the core structure is nearly independent of uncertainties in the helium-burning rate, since the central temperature goes as this rate to a very small (fractional) power. While the chosen value of the reduced alpha width of the 7.12 MeV level in O^{16} affects the final abundance of oxygen (§ V), it has little effect on the evolutionary track on the H-R diagram (cf. Iben's sequence *D* for $\theta_\alpha^2 \sim 0.1$ and *E* for $\theta_\alpha^2 \sim 1$ in Fig. 1).

In the hydrogen shell, we assumed that (1) oxygen is in equilibrium in the CNO cycle;

(2) the shell is infinitely thin with a discontinuity in luminosity and hydrogen abundance; and (3) outward burning of the shell during the earlier, rapid phase of gravitational contraction in the core can be neglected. For example, assumption (1) may not be justified everywhere in the shell region because the temperature is not high over a sufficiently broad domain and for a sufficiently long time prior to helium burning. These three assumptions may be tested by modifying the CNO abundance and by arbitrarily altering the shell mass fraction. Actual calculation shows that little change takes place on the H-R diagram, as anticipated by Hayashi and Cameron (1962) and by Hayashi, Hōshi, and Sugimoto (1962). However, the trends are for an increase of effective temperature with increasing shell mass fraction and with decreasing CNO abundance.

c) Chemical Composition

The models are rather sensitive to the initial chemical composition. The sensitivity considered here arises from the hydrogen and helium abundances which affect the mean molecular weight and the electron-scattering opacity. The model for 15.6 $M_\odot$ calculated by Hayashi and Cameron (1962) had $X_e = 0.90$, $Y_e = 0.08$, and $Z_e = 0.02$ (with assumptions similar to those we used). From their results, the trends which might be expected on homology arguments are given confirmation, namely, that a lower helium abundance causes a lower luminosity and a lower effective temperature (sequence F in Fig. 1).

We have recalculated the Hayashi-Cameron "turnback" model ($Y_c \sim 0.3$) with the inclusion of bound-free absorption. The effective temperature becomes at least 8500° K at the hottest point on the helium-burning track (assuming, at worst, that envelope convection covers *less* than 58 per cent of the mass in the previous red-supergiant phase) Therefore it appears likely that for any reasonable initial chemical composition, a star of 15 $M_\odot$ will spend some of its helium-burning lifetime as a blue supergiant.

d) Mass Loss

Mass loss is another effect to be taken into account in obtaining reliable initial models for helium burning. Underhill (1960) has estimated the rate of mass loss from a Be star to be 10^{-7} $M_\odot$/yr. This is comparable with the rate estimated also for B supergiants (Lucy and Solomon 1967). Consequently, we can obtain an upper limit to the amount of mass lost by assuming that the same rate holds for a B star during its main-sequence phase. For example, a star of initially 16 $M_\odot$ burns hydrogen for 1×10^7 yr until the onset of helium burning in the core. Losing mass at the above rate, it arrives at the helium-burning stage with 15 $M_\odot$ and interior zonal boundaries at roughly $q_0 = 0.500$ and $q_s = 0.245$ (cf. Stothers 1965). These are not very different from the boundaries in a star of 15 $M_\odot$ evolving at constant mass. Since the main-sequence mass-loss rate for normal B stars is probably closer to 10^{-8} $M_\odot$/yr (Underhill as quoted in Stothers 1963*b*), the amount of mass lost is probably quite negligible.

When the star is a red supergiant during the early stages of helium burning, the mass-loss rate may be 10^{-8} to 10^{-6} $M_\odot$/yr (Deutsch 1956; Weymann 1962). However, the lifetime here is less than 1×10^6 yr. Possibly mass loss may again be neglected. If not, it will have the effect of delaying the transition into the blue-supergiant region (Hayashi, Hōshi, and Sugimoto 1962).

IV. INVESTIGATION OF 60 $M_\odot$ AND 100 $M_\odot$

The models for 60 and 100 $M_\odot$ with only electron-scattering opacity (Table 2) behave like the analogous models for 15 $M_\odot$.

When the contribution from bound-free absorption is included in the opacity for the models of 60 $M_\odot$ (with an intermediate zone of varying composition), it is found to be quite small—even in the outermost layers it is less than 30 per cent of the total opacity. Nevertheless, the sensitivity of these very luminous, centrally condensed structures to

a varying opacity in the outer regions causes *all* the formally unmixed models of highest mass to have very low surface temperatures. Convective mixing must therefore occur at the outset. It will extend downward from the surface to some point between q_0 and q_s until the partial homogenization of the intermediate zone causes the star to move rapidly into the region of blue supergiants. The depth in mass fraction to which convection extends will be much smaller than in the case of 15 $M_\odot$ since (1) the intermediate zone is closer to the surface; and (2) bound-free absorption is a smaller fraction of the total opacity in the higher masses. Because of these effects, the stars of significantly higher mass than 15 $M_\odot$ are expected to remain red supergiants for a much briefer period during the onset of helium burning.

TABLE 2

SELECTED MODELS FOR 60 $M_\odot$ AND 100 $M_\odot$ DURING CORE HELIUM DEPLETION WITH PURELY ELECTRON-SCATTERING OPACITY*

	60 $M_\odot$†					100 $M_\odot$‡				
	1	2	3	4	5	1	2	3	4	5
q_s	0 426	0 490	0 508	0 509	0 506	0 482	0 545	0 552	0 552	0 549
X_s ..	0 030	0 173	0 212	0 315	0 311	0 030	0 159	0 173	0 249	0 243
L_H/L	0 447	0 224	0 087	0 032	0 028	0 331	0 103	0 045	0 006	0 005
q_4	0 335	0 414	0 448	0 459	0 462	0 405	0 488	0 504	0 514	0 515
Y .	0 970	0 641	0 282	0 0677	0 0127	0 970	0 492	0 276	0 0700	0 0100
X_C .	0 000	0 309	0 532	0 421	0 284	0 000	0 412	0 503	0 379	0 232
log T_c	8 307	8 335	8 379	8 440	8 497	8 328	8 369	8 397	8 456	8 520
log ρ_c	2 499	2 525	2 629	2 802	2 972	2 367	2 442	2 519	2 689	2 882
log $(L/L_\odot)$	6 071	6 069	6 071	6 076	6 080	6 388	6 387	6 389	6 393	6 397
log T_e .	4 178	4 375	4 396	4 324	4 250	4 191	4 345	4 329	4 217	4 107
τ (10^6 yr) .	0 00	1 01	2 13	3 04	3 38	0 00	1 20	1 82	2 61	2 94

* Neglect of κ_a and of previous envelope mixing makes the effective temperatures unreliable.

† 60 $M_\odot$: $\kappa = \kappa_s$; $q_0 = 0\ 759$; $X(q) = -1\ 094 + 2\ 99q - 0\ 825q^2$ or semiconvection.

‡ 100 $M_\odot$: $\kappa = \kappa_s$; $q_0 = 0\ 847$; $X(q) = -1\ 122 + 2.71q - 0\ 660q^2$ or semiconvection.

Calculation indicates, furthermore, that the more massive stars will attain hotter effective temperatures than their counterparts at 15 $M_\odot$. (Nevertheless, the *shape* of their evolutionary tracks ought to be similar.) On the extreme assumption of complete envelope homogenization ($q_s = 0.43$ and $X_s = X_e = 0.51$), a star of 60 $M_\odot$ evolves during helium burning at nearly constant luminosity and effective temperature (30000° K). A lesser amount of envelope homogenization produces cooler effective temperatures.

V. CORE EVOLUTION

During the early part of helium burning, the convective core expands, reducing the central density. However, at sufficiently high mass, the nuclear-energy generation is no longer able to resist perceptibly the high gravity. This occurs somewhere between 45 and 60 $M_\odot$. In the case of core hydrogen burning, it occurs between 20 and 30 $M_\odot$ (Stothers 1965).

The final abundances of carbon and oxygen in the core at helium exhaustion are found to be not highly sensitive to the stellar mass. For the reduced alpha width of the 7.12 MeV level in O^{16}, we have used $\theta_a^2 = 0.1$. This is within the probable error of 50 per cent attached to the rather uncertain theoretical value recently determined by Stephenson (1966). Our chosen value of θ_a^2 yields the following final carbon abundances:

$$M/M_\odot\text{: } 15, \quad 60, \quad 100;$$
$$X_C\text{: } 0.33, \quad 0.25, \quad 0.20\ .$$

These abundances are larger than those obtained by Deinzer and Salpeter (1964) for massive stars composed initially of pure helium, using the same value of θ_a^2. The reason is the lower central temperature of our models, caused by the presence of the hydrogen envelope.

Unless $\theta_a^2 \gtrsim 0.3$, massive stars are expected to experience a subsequent carbon-burning ($C^{12} + C^{12}$) phase.

VI. HELIUM-BURNING LIFETIME

As helium burning proceeds in the core, the contribution to the luminosity from the hydrogen shell source diminishes. Simultaneously, the mass fraction q_4 of the convective core boundary grows until it nearly overtakes the mass fraction q_s of the shell source.

In the limit of very high stellar masses (if we ignore bound-free absorption and mixing in a red-supergiant phase), the hydrogen shell does not burn at all, and q_4 is constant and equal to q_s, which is simply the convective core boundary at hydrogen exhaustion, viz., $(1 + X_e)^{-1}$. The explanation for this behavior in the limit is, first, the constancy of opacity in the core during helium burning and, second, the constancy of luminosity during the evolution of extremely massive stars (Stothers 1966*b*).

The lifetime of core helium burning is given by

$$\tau = \int (EM/L) d\bar{Y} ,$$

where $E = 6 \times 10^{17}$ ergs/g. In the limit of extremely massive stars, $L = 4\pi cGM/\kappa_e$ and $\Delta\bar{Y} = (1 - Z_e)q_s$. Consequently, the lower bound on the lifetime is

$$\tau = \frac{E}{4\pi cG} \frac{\kappa_e (1 - Z_e)}{1 + X_e} .$$

Since $\kappa_e/(1 + X_e)$ is a constant, the lifetime is *independent* of the initial hydrogen content. Thus $\tau/(1 - Z_e) = 0.144$ million years. For our chosen initial composition, $\tau = 0.140$ million years.

In the limit of very high masses, the ratio τ_H/τ_{He} of the hydrogen-burning lifetime to the helium-burning lifetime becomes a constant. For an initial composition of pure hydrogen, $\tau_H/\tau_{He} = 15$. For our chosen initial composition, $\tau_H/\tau_{He} = 9.7$. In the range 15–100 $M_\odot$, our computed models give a ratio $\tau_H/\tau_{He} \sim 9$.

VII. EVOLUTION ON THE H-R DIAGRAM

Since the evolution of a real star of 15 $M_\odot$ (with $X_e = 0.70$ and $Z_e = 0.03$) is tentatively expected to lie somewhere between the extremes represented by our two assumptions regarding the depth of the convective zone, we may draw the following conclusions. The star definitely initiates core helium burning as a red supergiant. It may spend less than a quarter of its helium-burning lifetime there. It crosses the Hertzsprung gap very rapidly and burns helium during the major portion of its lifetime as a blue supergiant. Its effective temperature ought to reach a maximum value somewhere between 15000° and 25000° K. Subsequently, the star recrosses the Hertzsprung gap on a fast (gravitational) time scale to initiate helium shell burning around a contracting carbon-oxygen core.

This scheme of evolution from a red supergiant to a blue supergiant is the result predicted by our models, but it neglects possible complications incurred during the convective-envelope phase. These complications may arise from the uncertainties in the opacity, mixing length, surface boundary conditions, and CNO abundance, as well as from the fact that the convective envelope does not extend all the way to the hydrogen-burning shell. For example, Hofmeister (1967) calculated the helium-burning phase for 5 and 9 $M_\odot$ with two slightly different initial chemical compositions and found that in one case the star *never* became a blue supergiant. Since the structure of a star of 15 $M_\odot$ at the onset of helium burning is not qualitatively different from that of a star of lower mass,

it is possible that suitable choices of "free" parameters (including mass loss) could result in an evolutionary track which does not leave the red-supergiant region.

For masses much higher than 15 $M_\odot$, stars are expected to spend practically all their helium-burning lifetime as blue supergiants after a brief red-supergiant phase. The maximum effective temperature attained should be hotter if the mass is higher. At 60 $M_\odot$ it should lie in the range 20000°–30000° K.

We may rule out, however, the hotter extremes of the temperature ranges for 15–60 $M_\odot$ because these extremes correspond to a complete chemical homogenization of the stellar envelope, in which case the evolutionary track on the H-R diagram is practically a point. The large spectral interval in which are found blue supergiants of young galactic clusters like h and χ Persei suggests that some degree of chemical inhomogeneity exists in the envelope. Complete mixing of the star is obviously ruled out by the mere presence of the supergiants, and this persists up to the highest masses known. For example, the blue supergiant ζ^1 Sco (Code and Houck 1958) has a mass of about 60 $M_\odot$, as inferred from its luminosity and our models.

Previous studies of massive stars, in which electron scattering was assumed to be the sole opacity source (Hayashi and Cameron 1962; Stothers 1966*a*) or in which the unstable part of the envelope was assumed to be fully convective (Iben 1966*b*), indicated that such stars would only reach the red-supergiant region after helium is exhausted in the core. In fact, Hayashi, Hōshi, and Sugimoto (1962) attempted to explain the red supergiants in h and χ Persei as stars in the carbon-burning and later phases. However, with bound-free absorption included in the stellar opacity and with envelope instability treated semiconvectively, we suggest that both the blue supergiants and the red supergiants (at least some of them) are to be explained by core helium-burning models.

One of us (R. S.) has been supported by an NAS-NRC postdoctoral research associateship under the National Aeronautics and Space Administration. We would like to thank Dr. Robert Jastrow for his hospitality at the Institute for Space Studies.

REFERENCES

Code, A. D , and Houck, T. E. 1958, *Pub. A.S.P.*, **70**, 261.
Deinzer, W., and Salpeter, E. E. 1964, *Ap. J.*, **140**, 499.
Deutsch, A. J. 1956, *Ap. J.*, **123**, 210.
Hayashi, C , and Cameron, R. C. 1962, *Ap. J.*, **136**, 166.
Hayashi, C , Hōshi, R., and Sugimoto, D. 1962, *Progr. Theoret. Phys. Suppl.* (Kyoto), No 22
Hofmeister, E. 1967, *Zs. f. Ap.*, **65**, 164.
Iben, I. 1966*a*, *Ap J* , **143**, 505.
———. 1966*b*, *ibid* , p. 516.
Lucy, L. B., and Solomon, P. M. 1967, *A.J.*, **72**, 310.
Sakashita, S , Ôno, Y., and Hayashi, C. 1959, *Progr. Theoret. Phys.* (Kyoto), **22**, 830.
Schwarzschild, M 1958, *Structure and Evolution of the Stars* (Princeton: Princeton University Press).
Stephenson, G J., Jr. 1966, *Ap. J* , **146**, 950.
Stothers, R. 1963*a*, *Ap. J* , **138**, 1074.
———. 1963*b*, *ibid* , p. 1085.
———. 1965, *ibid* , **141**, 671.
———. 1966*a*, *ibid* , **143**, 91.
———. 1966*b*, *ibid.*, **144**, 959.
Underhill, A B. 1960, *Stellar Atmospheres*, ed J. Greenstein (Chicago: University of Chicago Press), p. 411.
Weymann, R. 1962, *Ap. J* , **136**, 844.